



## Effect of particle size variation of Ag nanoparticles in Polyaniline composite on humidity sensing

Madhavi V. Fuke<sup>a,\*</sup>, Prajakta Kanitkar<sup>a</sup>, Milind Kulkarni<sup>b</sup>, B.B. Kale<sup>b</sup>, R.C. Aiyyer<sup>a</sup>

<sup>a</sup> Center for Sensor Studies, Department of Physics, University of Pune, Pune 411007, India

<sup>b</sup> Centre for Materials for Electronics Technology, Panchavati, off Pashan Road, Pune 411008, India

### ARTICLE INFO

#### Article history:

Received 9 October 2009

Received in revised form 4 December 2009

Accepted 7 December 2009

Available online 14 December 2009

#### Keywords:

Particle size

Plastic optical fiber

Ag-Polyaniline nanocomposite

Relative humidity

### ABSTRACT

The results of synthesis of Ag-Polyaniline nanocomposite along with an investigation of optical fiber based humidity sensor using evanescent wave absorption spectroscopy are discussed. The sensor was fabricated using Ag-Polyaniline nanocomposite deposited on an optical fiber clad and tested in the range of 5–95% relative humidity (RH). Optimization of clad length (2–8 mm) was done and then particle size (15–30 nm) variation of silver nanoparticles in Polyaniline composite was studied for better performance of sensor. The effect of particle size on sensing humidity was investigated. The reduction of particle size, leads to a dramatic improvement in sensitivity and speed of response. The optimized clad length of 6 mm exhibits the better results for 15 nm particle size of Ag nanoparticles dispersed in Polyaniline. The sensor response is fully reversible having almost 1% of standard deviation. Response time of the sensor is 30 s with a slow recovery of 90 s.

© 2009 Elsevier B.V. All rights reserved.

### 1. Introduction

Industrial processes and human comfort, both, need to measure and control the humidity in the environment. In recent years, the need of humidity sensor has greatly increased because of its applications; in control of air conditioning, quality control of food products in a wide range of industries, paper and textile industries, optimal functioning of modern solid state electronic equipment, civil engineering etc. The operating conditions and requirements of humidity sensors depend on the field of application. Therefore, development of low cost humidity sensors with better specifications is required. Polymer (plastic) fibers have numerous advantages in short-haul applications over glass fibers. First and foremost it is more pliable i.e. having the ability of Plexiglas to warp and bend versus a plate of window glass. POF has a shorter bend radius, more flexible and resistant to damage than glass optical fiber due to its intrinsic material characteristics. It is easier to terminate, polish, and connect as well, which can reduce the cost of installation and maintenance. Also the plastic optical fiber has advantages such as low cost, ease of handling and immunity from electromagnetic interference [1–5]. The number of fiber optic humidity sensors employing different concepts has been reported in the literature. Point sensors have been reported

which use the end of the fiber coated with either a metal or dielectric film [6]. Special fibers with the cladding removed and replaced with porous silica or polymer are used by Ogawa et al. and Ronot et al. [7,8]. The spectral absorption of  $\text{CoCl}_2$  entrapped in gelatine or polymer host when coated on fiber is also used for gas sensing [9,10]. The polished clad of the fiber with an overlay of RH dependent refractive index material is reported by Bownass et al. The polymeric composites show a sudden change in the refractive index leading to different switching points for the sensor allowing them to respond at different humidity levels [11,12].

Polymers are identified as good candidates for practical applications, since they are compatible to oxides and ceramics and also can be used at room temperature [13–15]. Nanocrystalline materials have also been a subject of intense research in the recent years due to the unusual properties exhibited by them. Nanocomposites are characterized by the dispersion of nanosized metals like silver, copper or nickel or semiconductors within an inert matrix [16]. The dispersoids have a large surface to volume ratio. This makes them potentially attractive for sensing purposes because of innumerable surface sites offered for physisorption of water molecules. The synthesis of nanocrystalline nickel oxide by controlled oxidation of Nickel nanoparticles and their humidity sensing properties are discussed by Das et al. [17], whereas Pal et al. [18] have explored the possibilities of using nanocomposites containing silver particles grown within a glass barium titanate composite by an ion exchange process followed by reduction technique for humidity sensing. Nano-like Magnesium oxide films were studied as optical fiber humidity sensor by Shukla et al. [19] and Vijayan et al. [20]

\* Corresponding author. Tel.: +91 20 2569 2678; fax: +91 20 2569 1684.

E-mail addresses: [mfuke@physics.unipune.ernet.in](mailto:mfuke@physics.unipune.ernet.in), [madhavifuke@rediffmail.com](mailto:madhavifuke@rediffmail.com) (M.V. Fuke).

has reported optical fiber humidity sensor based on Co-Polyaniline nanocomposites.

The sensing mechanism can be affected by the particle size of the material. It is found that the Indium Tin Oxide ethanol gas sensor is having better sensitivity with finer particle size compared to larger one. [21]. Particle size and doping have also been reported [22] to influence the performance of SnO<sub>2</sub> gas sensors. Yamazeo and Miura [23] studied the effect of grain size on the sensitivity of SnO<sub>2</sub> gas sensors and concluded that the sensitivity to both CO and H<sub>2</sub> increased considerably as grain size was reduced. Particle size effect was studied on porous Sol–Gel doped cladding U-shaped optical fiber for measurement of critical micelle concentration by Singh and Ogita [24]. Test results show that the sensitivity of the small particle size porous sol–gel cladding U-shaped optical fiber in sensing region is higher than that of large particle size sol–gel cladding-based U-shaped.

The aim of the present study is to realize a plastic optical fiber-based relative humidity sensor with better sensitivity and operational range. An evanescent wave fiber optic humidity sensor is constructed by using Ag-Polyaniline nanocomposite with variable particle sizes of Ag in Polyaniline cladded on bare clad of multimode fiber. The effect of particle size variation of silver in polymeric composite is studied in brief.

## 2. Experimentation

### 2.1. Synthesis of Ag nanoparticles

The synthesis method used is a modified version of the one originally used by Reetz and Helbig for Pd nanoparticles [25,26]. The electrochemical method is suitable for the synthesis of metal nanoparticles. An inexpensive two electrode electrochemical cell was devised in which the anode is in the form of bulk metal sheet to be transformed into corresponding metal ions. Platinum in the form of foil serves as a cathode. The distance between the two electrodes was 0.5 cm and was kept fixed.

An electrolyte containing a mixture of 80 ml of acetonitrile and 20 ml of Tetrahydrofuran (THF) (ratio 4:1) along with 0.55 mg of capping agent viz. Tetraoctylammoniumbromide (TOAB) was used. The solvents used were freshly distilled. The experimental setup is shown in Fig. 1. Electrolysis was carried out at room temperature, under nitrogen atmosphere for few hours in constant current mode.

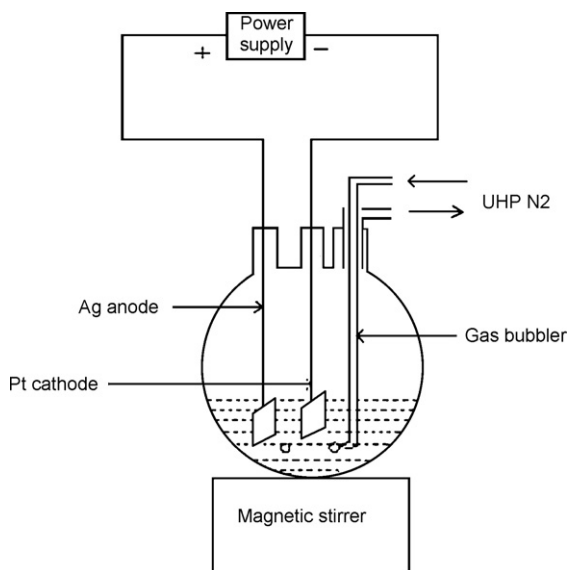


Fig. 1. Electrochemical cell for synthesis of metallic Ag nanoparticles.

A black precipitate of Ag nanoparticles settle down, whereby, a free flowing powder of Ag is obtained.

Initially the solvents i.e. acetonitrile and THF were taken in the electrochemical (E/C) cell and nitrogen bubbling was started with continuous stirring of solution. After about 6 h the capping agent i.e. TOAB was added to the E/C cell which dissolves immediately in the mixture of solvents. The electrolyte was continuously stirred using magnetic stirrer during the electrolysis period. Thus in the overall process the bulk metal (Ag) was oxidized at the anode. The Ag cations migrated to the cathode and reduction takes place with formation of Ag in zero oxidation state. Agglomeration with formation of undesired metal powder was prevented by the presence of the ammonium stabilizers.

The nanoparticles were separated by centrifugation and washed at least three times with acetonitrile. They were immediately vacuum dried at room temperature. The synthesized nanoparticles were dispersed in acetonitrile for further characterization.

### 2.2. Preparation of Ag-Polyaniline nanocomposite

All the chemicals and monomer used were of Analytical Reagents (AR) grade and used as received. The solutions were prepared using double distilled water. The polymerization was initiated by the drop wise addition of the oxidizing agent, (NH<sub>4</sub>)<sub>2</sub>S<sub>2</sub>O<sub>8</sub> (dissolved in minimum amount of water) in an acidified solution of monomer containing 50 wt.% of silver nanoparticles under constant stirring at 0–5 °C. Para toluene sulphonic acid (p-TSA) was used as a dopant, during the in-situ polymerization. The monomer to oxidizing agent ratio was kept as 1:1. After complete addition of the oxidizing agent, the reaction mixture was capped by stopper and kept under stirring for 24 h. The greenish black precipitate of the polymer was isolated by filtration and conditioned by washing and drying in an oven at 60 °C for 12 h. The solution so formed was further used for experimentation.

### 2.3. Working of Ag-Polyaniline Sensor

To fabricate Ag-Polyaniline-based humidity sensor, plastic optical fiber (POF) of length 30 cm was used. At the central portion of optical fiber, insulating cover was removed and then carefully the clad of the fiber was removed by heat treatment. This bare portion of the fiber was dip coated with Ag-Polyaniline nanocomposite to get humidity sensitive clad. This coated fiber was further bent to a 'U' shape with a bent radius of 10 mm taking into considerations the penetration depth considerations as reported by Gupta et al. [27] and Khijwania et al. [28]. The plastic optical fiber has a polymethylmethacrylate (PMMA) core of approximately 980 μm thickness, with 20 μm thick cladding made of fluoride containing carbon polymer. The refractive indices of the core and cladding were 1.492 and 1.417 respectively. The total diameter of the plastic optical fiber was 2.2 mm with PVC protecting sheath. The fiber end was wet polished with 600-grain sandpaper for predetermined time to maximize the optical power coupling to the plastic optical fiber. The ends of the plastic optical fiber were connected to a transmitter and receiver. Siemens PFC (plastic fiber components) emitters and detectors were used, which are low cost components. SFH450 emitter diode having a peak emission wavelength of 950 nm and a phototransistor SFH350 (responsivity of 0.3 μA/μW) was used as a transmitter and detector respectively. The advantage of the Siemens PFC's is the housing aperture into which a plastic optical fiber was introduced without having to remove the cladding, with an additional benefit of directly centering the fiber onto the transmitter and detector. A +5 V power supply was used to power the transmitter and the detector. The experimental setup is as shown in Fig. 2.

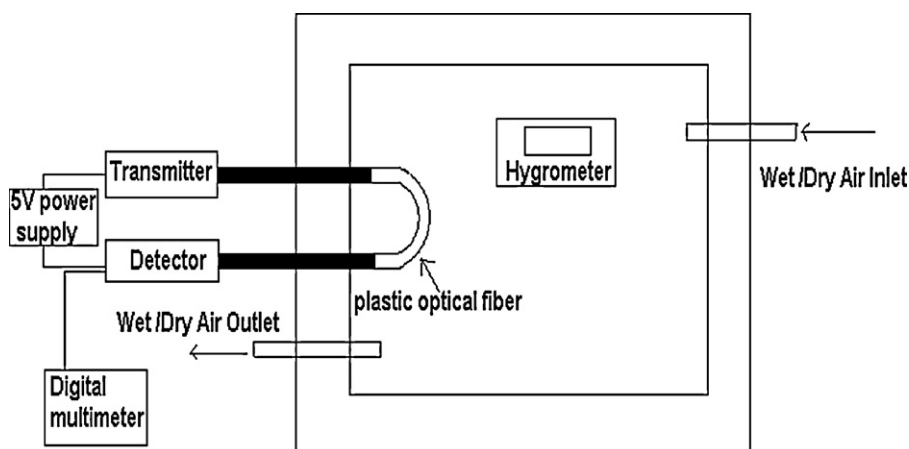


Fig. 2. Experimental setup for measurement of relative humidity.

A dome of 6 l capacity was used for RH measurement; values of RH were adjusted by proper inlet of wet/dry air at room temperature (25–30 °C). The transmitted output light intensity was measured with respect to relative humidity for various values of clad length and particle size of Ag in Polyaniline. First the length of cladding was optimized and then the particle size dependence was studied. The change in the %RH was measured directly, using a pre-calibrated hygrometer (Vaisala Humidity & Temperature Indicator HMI 31). The output voltage of the receiver (detector) as a result of change in humidity was measured using a Rishcom digital multimeter (Agilent DMM U1241A). The material characterization was done by X-Ray Diffraction (XRD) (for phases and size), UV–visible spectroscopy (UV), Fourier Transform Infrared Spectroscopy (FTIR) and Scanning Electron Microscopy (SEM).

#### 2.4. Structural characterization

X-Ray diffraction was performed with a Philips X-Ray diffractometer (CuK $\alpha$  as radiating wavelength). UV–vis spectra of the nanocomposites in acetonitrile were recorded by using Perkin Elmer spectrophotometer in the range of 200–800 nm. FTIR spectra of the samples were recorded on a Perkin Elmer-Spectrum 2000 spectrophotometer operated between 400 and 4000 cm<sup>-1</sup> in a KBr medium. The powder morphology of the composites in the form of film was investigated with an Analytical Scanning Electron microscope JOEL JSM 6360A.

### 3. Results and discussion

#### 3.1. XRD of Ag-Polyaniline nanocomposite

Generally Polyaniline is amorphous in nature and hence there are no sharp peaks found for Polyaniline. Literature study shows that Polyaniline is having peaks at 11°, 19°, 16° and 56°. Fig. 3 shows the XRD spectra of Ag-Polyaniline nanocomposite with variable sizes of silver nanoparticles where intense peaks having  $2\theta$  values of 26° and 56° correspond to the peaks for Polyaniline [29]. Especially the sharp peak at 26° (in our case) reveals the crystalline nature of the composite resulted due to the sequential growth of Polyaniline chain on the silver nanoparticles. Intense sharp peaks of silver sulphide are seen at  $2\theta$  values 35° and 37.2° with corresponding planes (0 2 2) and (1 0 3). Peaks corresponding to  $2\theta$  values 38.2° and 44.2° reveal the crystalline nature of silver in planes (1 1 1) and (2 0 0) respectively.  $2\theta$  values of 53.9° gives the corresponding peak of AgCl in (2 0 1) plane.

The particle size of silver nanoparticles is calculated from XRD with the help of Scherer formula. Fig. 3 shows the variation of particle size of silver nanoparticles where the peak intensity is shifting as per the particle sizes. As particle size increases, XRD peak height increases for the same material [30].

#### 3.2. UV–visible spectra of Ag-Polyaniline nanocomposite

Fig. 4 shows UV–vis absorption spectra of Ag-Polyaniline nanocomposite for different silver particle sizes. The absorption peaks around 400–420 nm originating from the surface plasmon resonance absorption of nanosized silver particles. UV–visible spectra show that the prominent peak of silver is shifting from 420 to 400 nm with decrease in particle size. Particle size reduction is supported by shift in absorption peak from blue to red region of wavelength [31]. Thus for bigger particle size of silver (30 nm), the absorption peak is found at 420 nm and for smaller particle size (15 nm) that is shifting towards 400 nm.

#### 3.3. FTIR of Ag-Polyaniline nanocomposite

Fig. 5 shows the FTIR spectra of Ag-Polyaniline nanocomposite for variable sizes of silver nanoparticles. The peak observed

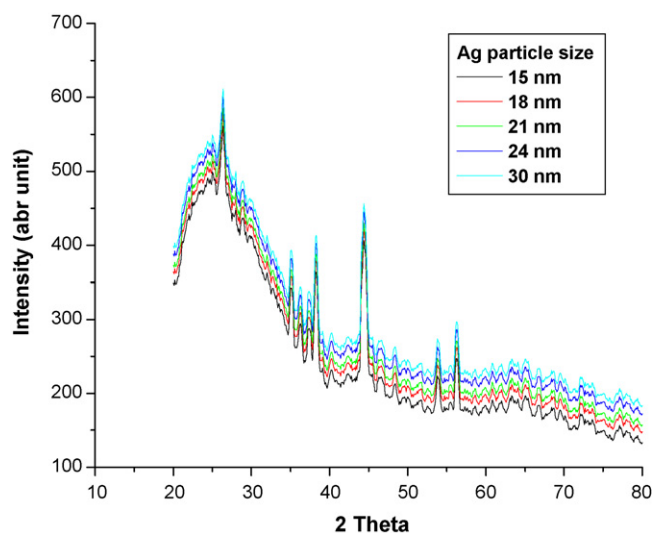


Fig. 3. XRD spectrum of Ag-Polyaniline nanocomposite for variable sizes of Ag.

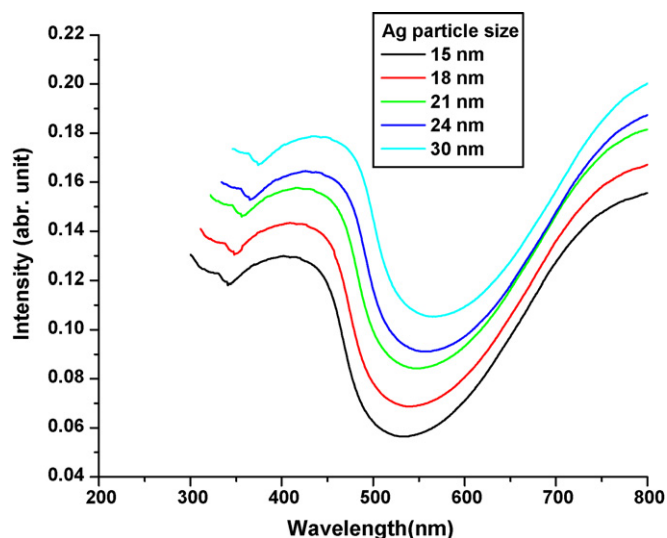


Fig. 4. UV-vis spectra of Ag-Polyaniline nanocomposite with Ag particle size variation.

at  $812.90\text{ cm}^{-1}$  is the characteristic of paradi-substituted aromatic rings indicating polymer formation. C–H in plane and C–H out of plane, bending vibrations appear at  $1122.58$  and  $683.87\text{ cm}^{-1}$ , respectively. Aromatic C–N stretching indicating appearance of the secondary aromatic amine group is observed at  $1303.22\text{ cm}^{-1}$ . Of particular interest are the bands in the vicinity of  $1399.07$  and  $1586.88\text{ cm}^{-1}$  corresponding to the benzoid ring and quinoid ring modes respectively. The presence of these bands clearly shows that the polymer is composed of insulating and conducting phase of the polymer. Band at  $3437.08\text{ cm}^{-1}$  is assigned to N–H stretching vibrations. Band at  $2922.21\text{ cm}^{-1}$  is assigned to aromatic C–H stretching vibration. The conducting ES phase of the polymer is confirmed by the presence of these characteristic bands. The metal oxygen stretching frequency of Ag–O is at  $567\text{ cm}^{-1}$ .

The FTIR spectra of variable particle sizes of Ag dispersed in Polyaniline shows that as the particle size decreases, the FTIR spectrum is shifting downwards [32]. Thus these FTIR spectra are supporting to the variable sizes of silver nanoparticles.

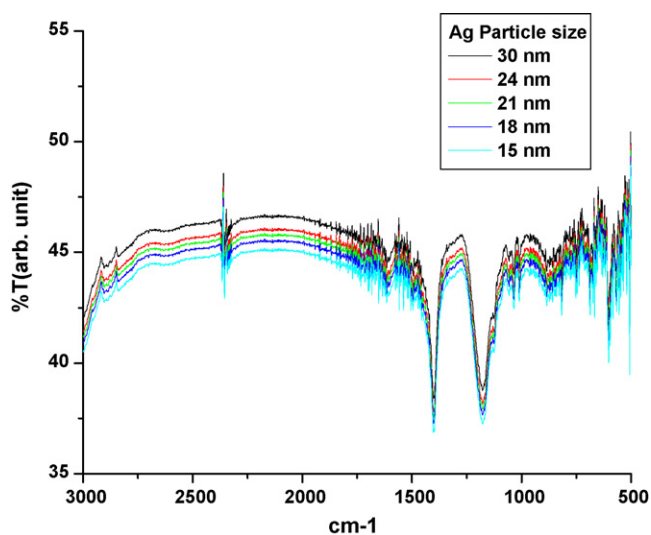


Fig. 5. FTIR spectra of Ag-Polyaniline nanocomposites with Ag particle size variation.

### 3.4. SEM of Ag-Polyaniline nanocomposite

The SEM micrographs of the films of Ag-Polyaniline nanocomposites of various particle sizes are as shown in Fig. 6. The grains structures are observed. For lower particle sizes the sponge like structures are observed. As the particle size increases, the films appear more compact. With increasing particle size the porosity decreases. For lower particle sizes (Fig. 6(a) and (b)) film appears to be more porous. Such composites are likely to facilitate adsorption of water vapors because of the pores which help to sense humidity. For higher particle sizes (Fig. 6(c)–(e)) the porous nature of the films decreases with decrease in sensitivity.

## 4. Humidity response

Optical fiber-based Ag-Polyaniline humidity sensor works on the principle of the evanescent wave adsorption. As the electromagnetic wave in the form of incident light guided propagates through the sensing region, the optical power in evanescent tail of the propagating mode is absorbed with the change in the environmental parameter i.e. humidity. This results in a modulated output from the fiber, which is used as the criterion for detecting and determining the relative humidity in the surrounding environment. As there is difference between refractive indices of core and cladding, the light traveling through the fiber is divided into two parts. A small portion of the optical power in the guided modes extends to the cladding region and interacts with the clad and larger portion of the optical power is available in the sensing region. This light is interacting with the mediating reagent in the coated film which gives an outward shift in the peak intensity of the light travelling through the fiber. This phenomenon of sensing is also supported by bending of the fiber. The response of the optical fiber towards humidity is checked for bare i.e. PMMA based fiber. As PMMA itself is good sensing material for humidity, the correction for the same is done. The optical fiber has a core refractive index of 1.492 which is greater than the refractive index (1.413) of the coated film used. The core and clad refractive index difference results in more leaky radiation field which maintains total internal reflection in the cladding. This phenomenon confines more power in the cylindrical waveguide. For higher humidity the confinement of light in the fiber is more as the refractive index decreases with increase in the humidity and vice versa. The change in output with respect to change in input is known as sensitivity which increases with increase in humidity.

To study the Ag-Polyaniline-based humidity sensor in detail, several experiments for clad-length variation of optical fiber and particle size variation of Ag in polymeric nanocomposite were done. Fig. 7 shows the effect of variation of Ag-Polyaniline deposited clad of an optical fiber on humidity response. The length of deposited clad was varied from 2–8 mm. From Fig. 7 it is cleared that the clad with 6 mm length shows maximum sensitivity towards humidity. There is gradual increase in the sensitivity with increase in clad lengths upto 6 mm. This is because the increase in clad length causes availability of larger interacting area for adsorption of hydroxyl ions which causes increase in the sensitivity. Adsorption of water changes the transmission properties of nanocomposite films which lead to a change in the effective refractive index. As the evanescent tail has only a small fraction of power, a longer portion of fiber is needed to be coated to have an effective interaction of light with the nanocomposite and hence a detectable change at the output. Bending the fiber transfers power from the guided modes to the leaky modes, providing more power to interact with the nanocomposite in the sensing region. This results in high sensitivity with a relatively small interaction length [27,28]. Hence 6 mm of clad length was considered as an 'optimal length' which gives maximum confinement to the transmitting beam. Though the clad-length variation study shows 10 mm opti-

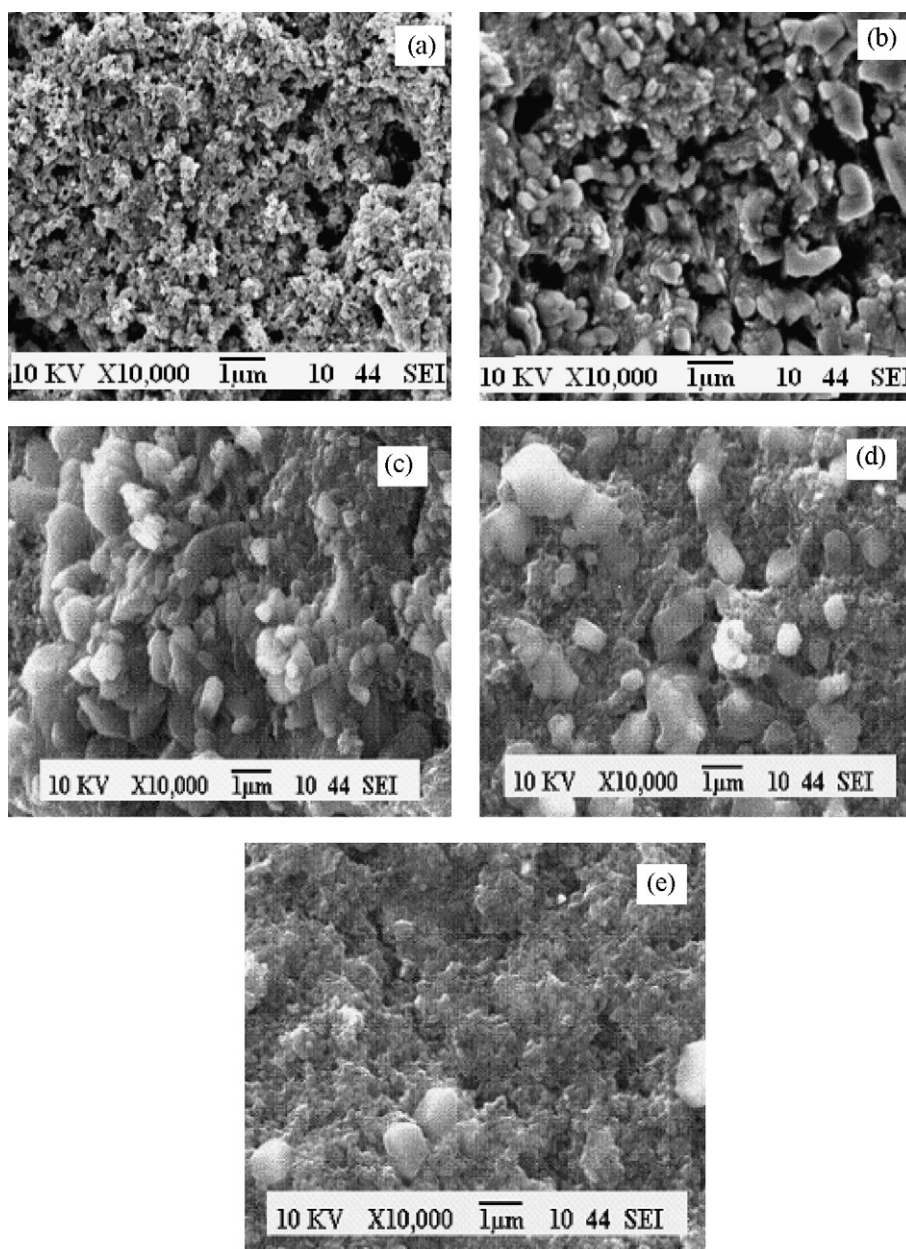


**Fig. 6.** Scanning Electron Micrograph (SEM) of Ag-Polyaniline nanocomposites for different Ag particle sizes (nm): (a) 15, (b) 18, (c) 21, (d) 24 and (e) 30.

mized clad length for Co-Polyaniline nanocomposites reported by Vijayan et al. [20], 6 mm is optimized for the Ag-Polyaniline nanocomposite. This variation in clad length is because the different material properties of the nanoparticles used as a cladding material. Because of the Co nanoparticles, more attenuation takes place in the transmitted light. Hence the active surface area available for sensing mechanism increases resulting in the large clad length of 10 mm for maximum sensitivity. The large surface area Ag nanoparticles require smaller active area for higher sensitivity applications. Hence the 6 mm of clad length is optimized for Ag-Polyaniline nanocomposite. Thus beyond the clad length of 6 mm, the sensitivity of this typical Ag-Polyaniline sensor decreases because of the decrease in confined light through the fiber. This might be happening due to the absorption of transmitted light by cladding material in addition to the obvious losses offered by the fiber which decreases the intensity relatively the sensitivity.

This optimized clad length was used for further experimentation for particle size variation (15–30 nm) of Ag nanoparticles in Polyaniline composite. Fig. 8 shows the response of particle size variation of Ag particles in Ag-Polyaniline nanocomposite for relative humidity sensor with better sensitivity. As the relative humidity increases, the sensitivity increases. The adsorption of water molecules on the film surfaces with large surface area and capillary pores increases the sensitivity. The water molecules adsorbed on the grain surface as well as in the pores. The Ag-Polyaniline films are having nanosized grains and pores which plays vital role in humidity sensing. The nanoscale grain size leads to much more grain boundaries and nanopores, leading to more active sites available for condensed water to react [33]. The higher surface area provides more sites for water adsorption and produces more charge carriers for electrical conduction [34]. From the graph it is cleared that as the particle size of the Ag nanoparticles decreases, the sensitivity of the sensor increases. Particle size of 15 nm shows

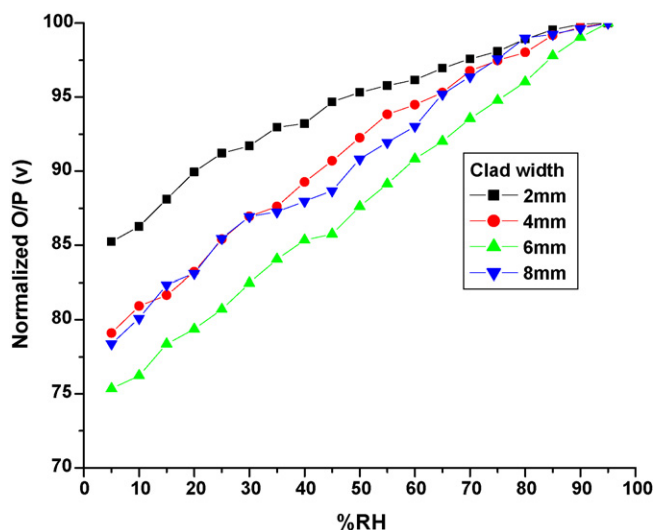


Fig. 7. Humidity response of Ag-Polyaniline nanocomposite for 2–8 mm clad lengths.

a maximum sensitivity (28.78 mV/%RH) for 6 mm clad length with almost linear fit of the plot. It is obvious that with increasing particle size, decreases the sites for adsorption of water molecules which reduces the sensitivity with respect to humidity.

This behavior is also supported by the SEM images shown in Fig. 6. The dispersion state of particles affects the performance of the sensor. But here the Ag nanoparticles are dispersed while polymerization of aniline. Hence more or less they are dispersed in the same way. From Fig. 6 it is cleared that the clad is more porous for small particle size. Hence smaller particle size of Ag nanoparticles offers more sites for interaction of water molecules offering maximum sensitivity. For higher particle size the numbers of voids are reducing which results in lower sensitivity for humidity. Due to the pores light penetrates deeper inside the clad elongating evanescent field of guide into clad. During this process some part of the light reflects back to the guide from clad-guide interface or scatters from the pores of the clad and overlaps with Evanescent Field (EF) of guide at the clad-guide interface. This maintains the coupling between the guide and clad. The smallest Ag particle size of 15 nm gives higher sensitivity

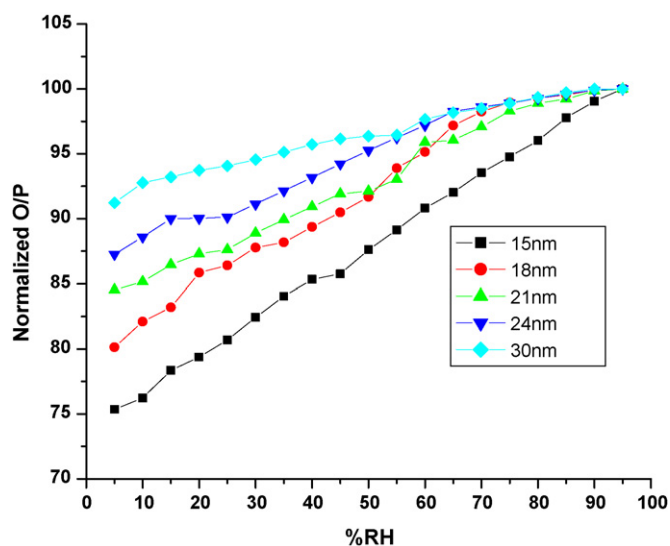


Fig. 8. Humidity response of Ag-Polyaniline nanocomposite for variable Ag particle sizes (15–30 nm) in polymeric composite for fixed clad length of 6 mm.

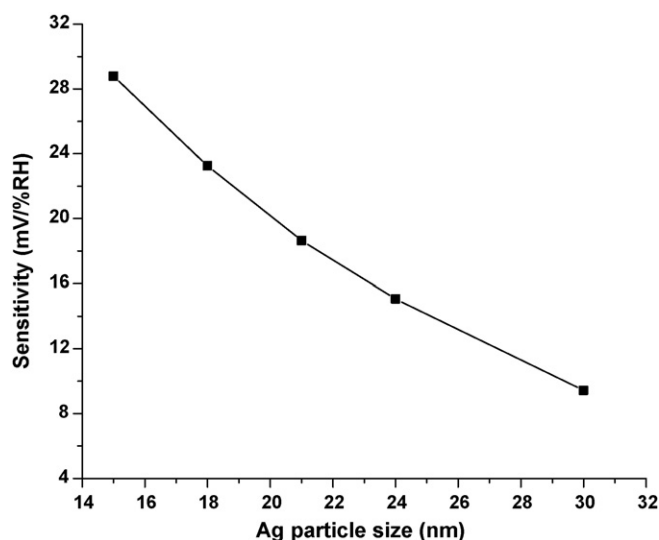


Fig. 9. Humidity response for variable particle sizes of Ag in Polyaniline nanocomposite at 5%RH.

towards humidity. This statement is supported by Fig. 9 which shows the response of variable particle sizes of Ag nanoparticles in Polyaniline composite for sensing humidity at fixed humidity of 5%RH.

Also concentration of the Ag particles plays a vital role in enhancing the sensitivity of the sensor [35]. For smaller particle size, surface to volume ratio decreases. Hence the number of particles in the same area increases. As conducting particle density increases, effectively sensitivity of the sensor also increases.

Small particle size of Ag in Polyaniline provides large number of sites for conduction mechanism. Due to its small size it appears to be having good mobility and hence has enhanced sensitivity. The smaller particle size gives larger specific surface area [21]. The water molecules first physically adsorb on the surface of the film and then penetrating inside the film. After penetration deep inside the film, chemisorptions take place. The dissociation of water molecule can be considered as surface reaction leading to the formation of surface oxides. This effectively changes the boundary conditions at cladding–guide interface increasing the beam confinement in the guide. Therefore, the output intensity through the cladded guide increases. The nanoparticles study states that for particular size of the nanoparticles, critical quantum confinement takes place. Because of this the properties of the material changes a lot. Hence for smaller Ag particle size (<15 nm) may the quantum confinement take place which may either increase or decrease the sensitivity of the sensor.

Interaction of water molecules with the film surface causes the sensing of humidity. The sensitivity curves of Ag-Polyaniline nanocomposite shows almost two regions of sensitivity. The two regions in sensitivity curves may be due to surface adsorption of the water vapors, being away from the actual guide will have lesser effect producing less sensitivity in lower humidity region and the diffusion of the vapors deep in the pores and adsorption on pore walls exhibiting higher sensitivity in higher humidity region. In this present case the physisorbed and chemisorbed water molecules add water refractive index (RI) enhancing the effective clad index. The increase in clad index enhances evanescent field (EF) and hence losses in the clad the initial RI of the clad are less than guide RI as required for optical fibers. These are higher than air RI therefore they offer higher transmission loss and leakier field in the clad. This leaky field increases with increase of clad RI and may be quite high as the clad RI goes beyond the guide RI at this point the radiation loss may be quite high.

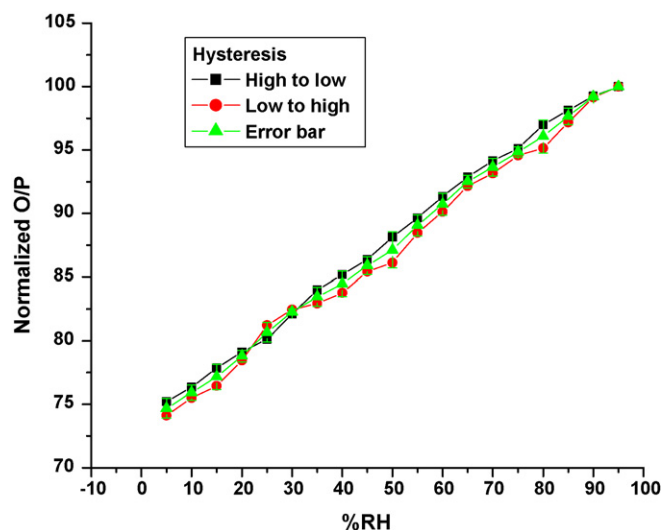


Fig. 10. Hysteresis curve of Ag-Polyaniline nanocomposite having 15 nm Ag particle size.

Addition of Ag nanoparticles plays great role in sensing humidity. When the film of Ag-Polyaniline was exposed to low humidity, sensitivity of the sensor is found to be low. This is because under dry conditions the polymer chains tend to curl up into a compact, coil form restricting the mobility of the Ag particles. On the other hand, at high humidity, polymer adsorbs water molecules and gets hydrated uncurling of the compact, coil form into straight chains that are aligned with respect to one another. Physisorption or chemisorption will change two parameters effectively viz. electrical conductivity and refractive index of the material. In this case the refractive index of the material of the clad changes with the relative humidity. The charge transfer or proton ion formation gives an increase in conductivity while the presence of water molecules in the film contributes towards the change in refractive index. The measurement of either parameter will give the response to the ambient in which the material is present [35].

The maximum difference in the two outputs (increasing and decreasing cycle) at the same RH level is defined as hysteresis. It is observed to be nearly 1% for all the particle sizes. Fig. 10 shows the hysteresis graph of the particle size of 15 nm. Slow desorption of the water from the pores of the capillary results in the hysteresis at lower humidity. The hysteresis and nonlinearity in the response is attributed to the capillary condensation which occurs at higher humidity, and forms a meniscus over the capillaries of the film.

The sensor shows quick response of 30 s (10–95% RH), recovery time of 90 s (95–10% RH). In this case the response is quite fast and recovery is slow.

## 5. Conclusions

The optical fiber clad of Ag-Polyaniline nanocomposite shows good response towards humidity with a wide range of 5–95%RH. Thus Ag-Polyaniline nanocomposite is a competent material for humidity sensing. Here a simple POF type optical humidity sensor

with a cladding layer of nanocomposites has been studied successfully, which is based on the POF structure change from leaky to guided, affected by the adsorption of water molecules. The particle size effect of silver nanoparticles is studied in brief. The smaller particle size facilitate adsorption more water molecules on the film surface. This sensor has a fast response of 30 s and recovery of 90 s.

## Acknowledgement

One of the authors, Madhavi Fuke would like to acknowledge Center for Sensor Studies, University of Pune, Pune for their financial support.

## References

- [1] C.D. Feng, S.L. Sun, H. Wang, C.U. Segre, J.R. Stetter, *Sens. Actuators B* 40 (1997) 217–222.
- [2] B.D. Gupta, Ratnanjali, *Sens. Actuators B* 80 (2001) 132–135.
- [3] B. Sorly, F. Pascal-Delannoy, A. Giani, A. Foucaran, *Sens. Actuators A* 100 (2002) 24–31.
- [4] C. Barian, I.R. Matis, F.J. Arregui, M. Lopez-Amo, *Sens. Actuators B* 69 (2000) 127–131.
- [5] S. Otuski, K. Adachi, T. Taguchi, *Sens. Actuators B* 53 (1998) 91–96.
- [6] F. Mitschke, *Opt. Lett.* 14 (1989) 967.
- [7] K. Ogawa, S. Tsuchiya, H. Kawakami, T. Tsutsui, *Electron. Lett.* 24 (1988) 42–43.
- [8] C. Ronot, M. Archenault, H. Gagnaire, J.P. Goure, N. Jaffrezic-Renault, T. Pichery, *Sens. Actuators B* 11 (1–3) (1993) 375–381.
- [9] A.P. Russell, K.S. Fletcher, *Anal. Chim. Acta* 170 (1985) 209–216.
- [10] D.S. Ballantine, H. Wohltjen, *Anal. Chem.* 58 (1986) 2883.
- [11] D.C. Bownass, J.S. Barton, J.D.C. Jones, *Opt. Lett.* 22 (5) (1997) 346–348.
- [12] D.C. Bownass, J.S. Barton, J.D.C. Jones, *Opt. Commun.* 146 (1998) 90–94.
- [13] Y. Li, M.J. Yang, N. Camaioni, G. Casalbore-Miceli, *Sens. Actuators B* 77 (2001) 625.
- [14] C.W. Lee, Y. Kim, S.W. Joo, M.S. Gomg, *Sens. Actuators B* 88 (2003) 21.
- [15] P.R. Somani, A.K. Viswanath, R.C. Aiyer, S. Radhakrishnan, *Sens. Actuators B* 1 (2001) 4054.
- [16] S. Banerjee, S. Banerjee, A. Datta, D. Chakravorty, *Europhys. Lett.* 46 (1999) 346–350.
- [17] D. Das, M. Pal, E.D. Bartolomeo, E. Traversa, D. Chakravorthy, *J. Appl. Phys.* 88 (2000) 6856–6860.
- [18] B.N. Pal, T.K. Kundu, S. Banerjee, D. Chakravorthy, *J. Appl. Phys.* 93 (2003) 4201–4206.
- [19] S.K. Shukla, G.K. Paraskar, A.P. Mishra, P. Mishra, B.C. Yadav, R.K. Shukla, L.M. Bali, G.C. Dubey, *Sens. Actuators B* 98 (2004) 5–11.
- [20] A. Vijayan, M. Fuke, R. Hawaldar, M. Kulkarni, D. Amalnerkar, R.C. Aiyer, *Sens. Actuators B* 129 (1) (2008) 106–112.
- [21] G.-Y. Cha, W.-W. Baek, S.-T. Lee, J.-O. Lim, J.-S. Huh, *J. Ceram. Soc. Jpn.* 112 (4) (2004) 252–258.
- [22] C.N. Xu, J. Tamaki, N. Miura, N. Yamazoe, *Sens. Actuators B* 3 (1991) 147–155.
- [23] N. Yamazoe, N. Miura, in: S. Yamauchi (Ed.), *Chemical Sensor Technology*, vol. 4, Kodansha, Tokyo, 1992.
- [24] C.D. Singh, M. Ogita, *Appl. Phys. B* 79 (2004) 389–391.
- [25] M.T. Reetz, W. Helbig, *J. Am. Chem. Soc.* 116 (1994) 7401.
- [26] M.T. Reetz, M. Winter, R. Brienbauer, T. Thurun-Albrecht, W. Vogel, *Chem. Eur. J.* 7 (2001) 1084.
- [27] B.D. Gupta, H. Dodeja, A.K. Tomar, *Opt. Quant. Electron.* 28 (1996) 1629–1639.
- [28] S.K. Khijwania, B.D. Gupta, *Opt. Quant. Electron.* 31 (1999) 625–636.
- [29] Madhavi V. Fuke, A. Vijayan, M. Kulkarni, R. Hawaldar, R.C. Aiyer, *Talanta* 76 (2008) 1035–1040.
- [30] G. Neri, A. Bonavita, G. Micali, G. Rizzo, N. Pinna, M. Niederberger, *J. Ba, Sens. Actuators B* 130 (1) (2008) 222–230.
- [31] A. Babapour, O. Akhavan, A.Z. Moshfegh, A.A. Hosseini, *Thin Solid Films* 515 (2006) 771–774.
- [32] R. Signorell, M.K. Kunzmann, M.A. Suhm, *Chem. Phys. Lett.* 329 (2000) 52–60.
- [33] P. Chauhan, S. Annapoorni, S.K. Tripathi, *Thin Solid Films* 346 (1999) 266–268.
- [34] K.S. Chou, T.K. Lee, F.J. Liu, *Sens. Actuators B* 56 (1999) 106–111.
- [35] N. Parvatikar, S. Jain, C.M. Kanamadi, B.K. Chougule, S.V. Bhoraskar, M.V.N. Ambika Prasad, *J. Appl. Polym. Sci.* 103 (2007) 653–658.